Automatic Fabric Inspection using GLCM-based Jensen-Shannon Divergence

V. Asha
E-mail: v_asha@live.com; asha.gurudath@gmail.com
Department of Master of Computer Applications, New Horizon College of Engineering, Bangalore, India
ORCID: 0000-0003-4803-099X

Keywords: cluster, co-occurrence matrix, defect, periodicity, Jensen-Shannon, divergence

Received: November 25, 2019

Jensen-Shannon divergence is one of the powerful information-theoretic measures that can capture mutual information between two probability distributions. In this paper, a machine vision algorithm is proposed for automatic inspection on dot patterned fabric using Jensen-Shannon divergence based on gray level co-occurrence matrix (GLCM). Input defective images are split into several periodic blocks based on their periodicities extracted using superposition of distance matching functions and the gray levels are quantized from 0-255 to 0-63 to keep the GLCM compact and to reduce the computation time. Symmetric Jensen-Shannon divergence metrics are calculated from the GLCMs of each periodic block with respect to itself and all other periodic blocks to get a dissimilarity matrix that satisfies true metrics conditions. This dissimilarity matrix is subjected to hierarchical clustering to automatically identify defective and defect-free blocks. Results from experiments on real fabric images with defects such as broken end, hole, thin bar, thick bar, netting multiple and knot show the effectiveness of the proposed method for fabric inspection.

Povzetek: Razvita je metoda, ki na osnovi Jensen-Shannovove divergence omogoča iskanje pokvarjenih vzorcev na ponavljajoči se shemi.

1 Introduction

Periodically patterned texture images are often found in day-to-day life in various applications such as ceramic tiles, wallpapers, and textile fabrics. Inspection of these products plays a major role with regard to quality control of the products in industries. Conventional human-vision based inspection are being followed in many of the industries. Lack of repeatability and reproducibility of inspection results due to fatigue and subjective nature of humans and imperfect inspection due to complicated design in the texture patterns are common in the conventional human-vision based inspection systems. Automated machine-vision based inspection can promote the production rate of the products by decreasing the inspection time compared to the traditional human-vision based inspection especially in industries such as textile industries. Periodic textures which we come across in our life include several natural patterns and made-made / artificial patterns. Plenty of patterns are used in textile fabric design. These patterns, in turn, include either random structures or periodic structures, making the fabric appealing to our eyes. Inspection on fabric images having periodic texture patterns is more complicated than that on plain and twill fabric images due to complexity in the design, existence of numerous categories of patterns, and similarity between the defect and background [1]. For the inspection on periodically patterned fabrics, there are methods in literature that depend on training stage with numerous defect-free samples for obtaining decision-boundaries or thresholds prior to detection of defects [1]-[11]. However, unsupervised method of identifying defects in a patterned texture image is quite challenging [12]-[17]. In this paper, a method of inspection on periodically patterned fabrics is proposed without any training stage with the help of texture-periodicity and Jensen-Shannon divergence metric based on gray level co-occurrence matrix. The main contributions of this research can be summarized as follows:

- There is no training stage with defect-free samples for decision boundaries or thresholds unlike other methods.
- Due to the absence of training stage with defect-free samples, the proposed method does not need huge memory space for storage of defect-free samples.
- Identification of defective and defect-free periodic units of the fabrics is automatically carried out based on cluster analysis without human intervention.

The program for the proposed algorithm is written in Matlab-7.0. The organization of this paper is as follows: Section-2 presents a brief review on Jensen-Shannon divergence, gray level co-occurrence matrix and the proposed algorithm for fabric inspection along with illustration and results from experiments on various real fabric images with defects. Section-3 has the conclusions.

2 Proposed algorithm for fabric inspection

Jensen-Shannon divergence is one of the effective measures for capturing mutual information between two probability distributions [12]. In this paper, it is intended to employ Jensen-Shannon divergence metric to discriminate between defective and defect-free periodic blocks as feature extraction (e.g. [18],[19]). Following the fact that human vision perception makes use of second-order statistics for texture discrimination [20], histogram constructed from second-order statistics is used to discern between defective and defect-free periodic blocks. Since the time of proposal of 14 features derived from histogram of second order statistics or gray-level co-occurrence matrices (GLCM) by Haralick *et al*. **[21]**, several authors have employed GLCM features for various texture analysis applications (e.g.[22]-[26]). Instead of extracting GLCM features, information from every pixel-pair of a periodic block with that of other periodic block is used to compute a distance metric using Jensen-Shannon divergence. The uniqueness of this Jensen-Shannon divergence metric based on GLCM is that the distance measure is considered for every pair of gray levels between two periodic blocks unlike the conventional GLCM features that are computed for the entire GLCM.

2.1 Brief review on Jensen-Shannon divergence

Jensen-Shannon divergence is a symmetrized, smoothed version of Kullback-Leibler divergence which is the most important divergence measure of information theory [18]. Given two classes $p(\omega_1)$ and $p(\omega_2)$ with a common feature vector *x*, the Kullback-Leibler divergence or the relative entropy in terms of ratio of the probability distributions of these classes conveys useful information concerning the capability of discriminating the two classes. This class-separability measure over class ω_1 is given as [27]

$$\lambda(\omega_1, \omega_2) = \int_{-\infty}^{\infty} p(\omega_1) log\left(\frac{p(\omega_1)}{p(\omega_2)}\right) dx \quad (1)$$

Similarly, the class-separability measure over class ω_2 is given as

$$\lambda(\omega_2, \omega_1) = \int_{-\infty}^{\infty} p(\omega_2) log\left(\frac{p(\omega_2)}{p(\omega_1)}\right) dx \quad (2)$$

Based on the probability distributions $p(\omega 1)$ and $p(\omega_2)$ and their average, a symmetric divergence called Jensen-Shannon divergence Λ is given as

$$\Lambda = \int_{-\infty}^{\infty} \left\{ p(\omega_1) \log\left(\frac{0.5 \times p(\omega_1)}{p(\omega_1)+p(\omega_2)}\right) + p(\omega_2) \log\left(\frac{0.5 \times p(\omega_2)}{p(\omega_1)+p(\omega_2)}\right) dx \right\} \quad (3)$$

Since Kullback-Leibler divergence λ (ω_1,ω_2) or λ (ω_1,ω_2) can be interpreted as the inefficiency of assuming that the true distribution is $p(\omega_2)$ or $p(\omega_1)$ when it is really $p(\omega_1)$ or $p(\omega_2)$, Jensen-Shannon divergence can be considered as a minimum inefficiency distance.

2.2 Brief review on Gray Level Co-occurrence Matrix

Gray level co-occurrence matrices (GLCM) have been employed in extracting texture features for various applications for a long time. It is a measure of gray-level dependencies in a local neighborhood for a given pixel displacement and orientation. In other words, a GLCM is a matrix showing the number of times a pixel with gray level *I* occurs at position vector from a pixel with gray level *j*. Mathematically, the GLCM for an image$I(x, y)$ of size (M, N) at a given offset $(\Delta x, \Delta y)$ is given as

$$C_{\Delta x,\Delta y} = \sum_{i=0}^{L-1} \sum_{j=0}^{L-1} \begin{cases} 1, if\ I(x,y) = i\ and \\ I(x+\Delta x, y+\Delta y) = j; \\ 0, otherwise. \end{cases} \quad (4)$$

where, L is the total number of gray values in the image. For an-bit image, the value of L is 2n with dynamic range of gray values being [0, L-1]. The offset (Δx, Δy) characterizes the pixel displacement and the orientation for the co-occurrence matrix.

2.3 Description of the algorithm

There are three major assumptions in the proposed algorithm as follows:

- Test image contains at least two periodic units in horizontal direction and two in vertical direction whose row and column dimensions are known a priori.
- Number of defective periodic units is always less than the number of defect-free periodic units.
- Test images are from imaging system oriented perpendicular to the surface of the product to be inspected. This assumption is due to the fact that in an inspection system in industries, the imaging system is always oriented perpendicular to the plane of the surface of the products such as tiles, wallpapers, and textile fabrics.

An image under inspection may have fractional periods also. Hence, the concept of analyzing the periodic blocks extracted from all four corners of the test image is used for identifying the defects followed by the concept of defect fusion proposed in [28]. Four cropped images are obtained from the defective test image by cropping the input image from all four corners (top-left, bottom-left, top-right and bottom-right) to get complete number of periodic blocks. If g is an image of size M × N with row periodicity P_r (i.e., number of columns in a periodic unit) and column periodicity P_c (i.e., number of rows in a periodic unit), size of the cropped images is M_{crop} × N_{crop}, where M_{crop} and N_{crop} are measured from top-left, bottom-left, top-right and bottom-right corners and are given by the following equations:

$$M_{crop} = floor\left(\frac{M}{P_c}\right) \times P_c \quad (5)$$

$$N_{crop} = floor\left(\frac{N}{P_r}\right) \times P_r \quad (6)$$

Each cropped image is split into several periodic blocks of size Pc x Pr. The periodicities are estimated using Superposition of distance matching function proposed in [29]. The decision that one has to make now

is how many levels are needed to construct a GLCM for effective texture analysis. The number of gray levels is an important factor in the computation of GLCM. The more levels included in the computation, the more accurate the extracted textural information, with, of course, a subsequent increase in computation costs and too less gray levels will result in loss of information due to quantization. In general, the effect of false-contouring starts predominating in an image if the gray levels are quantized below the dynamic range of gray values 0-63 [30]. In the proposed method, each 8-bit test image having a dynamic range of gray values 0-255 is linearly quantized to 6-bit image having a dynamic range 0-63 and rotation-invariant GLCMs (sum of GLCMs over 8 directions $\theta \in \{0, \pi/4, \pi/2, 3\pi/4, \pi, 5\pi/4, 3\pi/2, 7\pi/8\}$) calculated for a unit pixel displacement is utilized. If p(i, j) and q(i, j) represent the summed up GLCMs of two periodic blocks A and B respectively whose dynamic range of gray values is between 0 and L-1 for a unit pixel displacement, the Jensen-Shannon divergence can be computed as

$$\Lambda_{A,B} = \Lambda_{B,A} = \sum_{i=0}^{L-1}\sum_{j=0}^{L-1}\left\{p(i,j)\log\left(\frac{0.5\times p(i,j)}{p(i,j)+q(i,j)}\right)+q(i,j)\log\left(\frac{0.5\times q(i,j)}{p(i,j)+q(i,j)}\right)\right\} \quad (7)$$

The square root of this divergence is a true metric obeying the conditions of a true metric in 2D Euclidean space [18], viz.,$\sqrt{\Lambda_{i,j}} \geq 0$ for all i and j (non-negativity), $\sqrt{\Lambda_{i,j}} = 0$ for all $i = j$ (self-distance) and $\sqrt{\Lambda_{i,j}} = \sqrt{\Lambda_{j,i}}$ for all i and j (symmetry), and $\sqrt{\Lambda_{i,j}} \leq \sqrt{\Lambda_{i,k}} + \sqrt{\Lambda_{k,j}}$ for $i \neq j \neq k$ (triangular inequality). Following Eq. (7) based on Jensen-Shannon divergence for each periodic block with respect to itself and all other periodic blocks, a dissimilarity matrix D containing true distance metrics can be obtained as below:

$$D = \begin{pmatrix} \sqrt{\Lambda_{1,1}} & \sqrt{\Lambda_{1,2}} & \cdots & \sqrt{\Lambda_{1,n-1}} & \sqrt{\Lambda_{1,n}} \\ \sqrt{\Lambda_{2,1}} & \sqrt{\Lambda_{2,2}} & \cdots & \sqrt{\Lambda_{2,n-1}} & \sqrt{\Lambda_{2,n}} \\ \vdots & \vdots & \vdots & \vdots & \vdots \\ \sqrt{\Lambda_{n-1,1}} & \sqrt{\Lambda_{n-1,2}} & \cdots & \sqrt{\Lambda_{n-1,n-1}} & \sqrt{\Lambda_{n-1,n}} \\ \sqrt{\Lambda_{n,1}} & \sqrt{\Lambda_{n,2}} & \cdots & \sqrt{\Lambda_{n,n-1}} & \sqrt{\Lambda_{n,n}} \end{pmatrix} \quad (8)$$

It should be noted that if a cropped image has n number of periodic blocks, then the size of the dissimilarity matrix is n x n. Because the divergence measure of a periodic block with itself is zero and the divergence measure between ith periodic block and jth periodic block is same as the divergence measure between jth periodic block and ith periodic block, the dissimilarity matrix becomes a diagonally symmetric matrix with diagonal elements being zero as below:

$$D = \begin{pmatrix} 0 & & & & \\ \sqrt{\Lambda_{2,1}} & 0 & & & \\ \vdots & \vdots & \vdots & & \\ \sqrt{\Lambda_{n-1,1}} & \sqrt{\Lambda_{n-1,2}} & \cdots & 0 & \\ \sqrt{\Lambda_{n,1}} & \sqrt{\Lambda_{n,2}} & \cdots & \sqrt{\Lambda_{n,n-1}} & 0 \end{pmatrix} \quad (9)$$

It may be noted that because the matrix is similar about the diagonal, the upper diagonal elements are not filled for the sake of simplicity. This dissimilarity matrix is directly given as input to the Ward's cluster algorithm [28],[31] to automatically get defective and defect-free periodic blocks from each cropped image. Detection of defective periodic blocks from each cropped image does not give an overview of the total defects in the input defective image. Hence, in order to get the overview of the total defects in the input image, defect-fusion proposed in [28] is used which involves fusion of the boundaries of the defective periodic blocks identified from each cropped image, morphological filling and Canny edge extraction.

2.4 Illustration of the algorithm

In order to illustrate the proposed algorithm for fabric inspection, let us a defective box-patterned fabric image as shown in Fig. 1 (a). Following Eqs. (5) and (6), four cropped images containing complete number of periodic blocks are obtained as shown in Fig. 1 (b) - (e), from the test image with the help of periodicities known a priori.

Each cropped image is split into several blocks of size same as the size of the periodic unit and the gray values are quantized from 0-255 to 0-63. Jensen-Shannon divergence metrics are calculated for each periodic block with respect to itself and all other periodic blocks and a dissimilarity matrix is obtained from the GLCMs calculated over 8 directions for unit pixel displacement. The dissimilarity matrices thus obtained are shown in Fig. 2 in gray-scale form by scaling the matrix elements linearly in the range 0-255. Dark pixels indicate closeness among the periodic blocks and bright pixels indicate high dissimilarity. It may be noted from Fig. 2 that the diagonal elements in the dissimilarity matrix clearly indicate that the periodic blocks are of zero dissimilarity with themselves and that the dissimilarity matrix is symmetric.

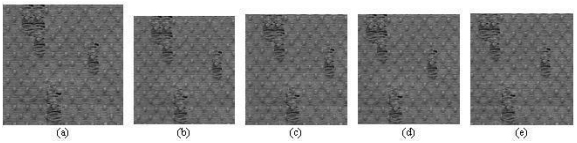

Figure 1: (a) Input defective image; (b) Cropped image obtained from top-left corner of the input image; (c) Cropped image obtained from bottom-left corner of the input image; (d) Cropped image obtained from top-right corner of the input image; (e) Cropped image obtained from bottom-right corner of the input image.

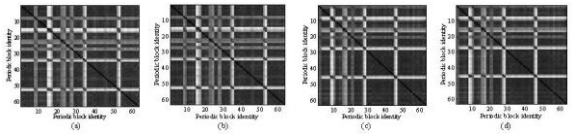

Figure 2: Dissimilarity matrix derived from the Jensen-Shannon divergence metrics for the cropped image obtained from (a) top-left (b) bottom-left (c) top-right and (d) bottom-right corners of the test image shown in gray-scale.

The dendrograms obtained from the dissimilarity matrices through Ward's hierarchical clustering are shown in Fig. 3 along with the defective periodic blocks identified by the clustering for all cropped images. Boundaries of the defective periodic blocks thus identified from each cropped image are highlighted using white pixels and shown in Fig. 4. Boundaries of the defective periodic blocks identified from each cropped image are shown superimposed on the original image in Fig. 5 (a) and separately on a plain background in Fig. 5 (b). Fig. 5 (c) shows the result of morphological filling and Fig. 5 (d) shows the edges of the total defects superimposed on the original defective image after Canny edge detection. Thus, an overview of the total defects on the original image itself can be obtained following the concept of fusion, morphological filling and edge detection. It may be noted that though the number of periodic blocks taken from a defective input image is same for all of its cropped images, the number of defective periodic blocks identified does not need to be same for all cropped images. This is because the contribution of defect in each periodic block may differ for different cropped images. Nevertheless, fusion of defects from all 4 cropped images helps in getting an overview of total defects in the input image. This is clearly evident from the example image used for illustration of the proposed algorithm.

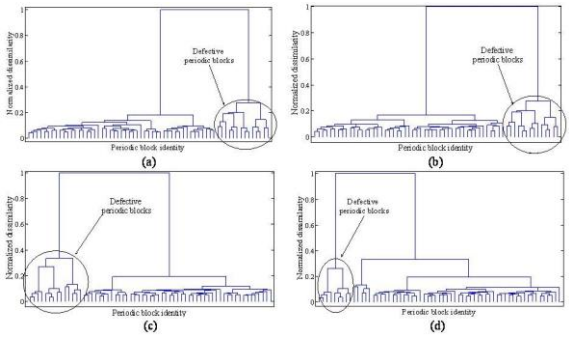

Figure 3: Dendrogram obtained from cluster analysis of the matrix containing Jensen-Shannon divergence metrics obtained from the test image by cropping it from (a) top-left (b) bottom-left (c) top-right and (d) bottom-right corners. Defective blocks identified from these cropped images are (8, 16, 27, 9, 17, 28, 24, 35, 53, 15, 34, 52, 22, and 23), (8, 16, 27, 24, 35, 53, 9, 17, 28, 15, 34, 52, 22, and 23), (28, 46, 17, 9, 8, 27, 45, 15, 16, 1, 20, 2, 10, and 21) and (28, 46, 17, 9, 8, 27, 45, 15, and 16).

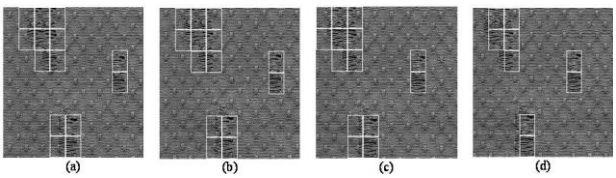

Figure 4: Defective periodic blocks identified from the cluster analysis of dissimilarity matrix derived from the Jensen-Shannon divergence metrics of the cropped images obtained from (a) top-left (b) bottom-left (c) top-right and (d) bottom-right corners of the test image with their boundaries highlighted using white pixels.

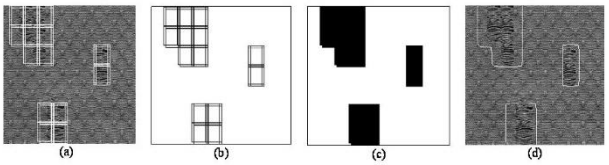

Figure 5: Defective periodic blocks identified from the cluster analysis of dissimilarity matrix derived from the Jensen-Shannon divergence metrics of the cropped images obtained from (a) top-left (b) bottom-left (c) top-right and (d) bottom-right corners of the test image with their boundaries highlighted using white pixels. Illustration of defect fusion: (a) Boundaries of the defective blocks identified from each cropped image shown super-imposed on the original image; (b) Boundaries of the defective blocks shown separately on plain background; (c) Result of morphological filling; (d) Edges identified through Canny edge operator shown superimposed on original defective image using white pixels.

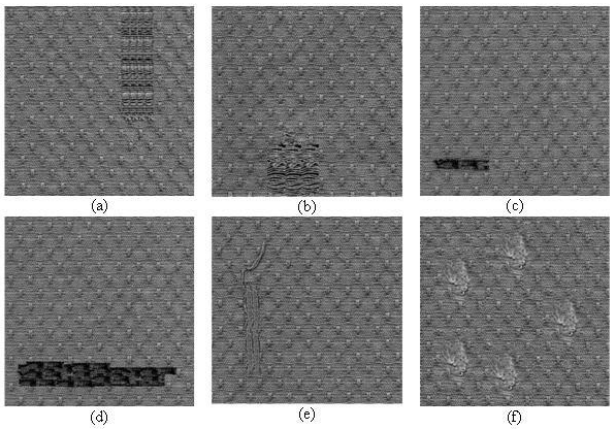

Figure 6: Sample fabric images with defect - (a) broken end, (b) hole, (c) thin bar, (d) thick bar, (e) netting multiple, and (f) knot.

2.5 Experiments on real fabric images with different types of defects

Periodically patterned fabric images with defects such as broken end, thin bar, thick bar, netting multiple and knot are tested to study the performance of the proposed algorithm of fabric inspection. Fig. 6 shows the defective fabric images and Fig. 7 shows the final result of defect identification after fusion, morphological filling and edge detection.

2.6 Performance evaluation and comparison with other methods

Precision, recall and accuracy are the widely used performance parameters in several retrieval applications. In order to access the performance of the proposed method, these performance parameters are evaluated in terms of true positive (TP), true negative (TN), false positive (FP), and false negative (FN), [31], [33], [34], [35]. True positive is defined as the number of defective periodic blocks identified as defective. True negative is defined as the number of defect-free periodic blocks

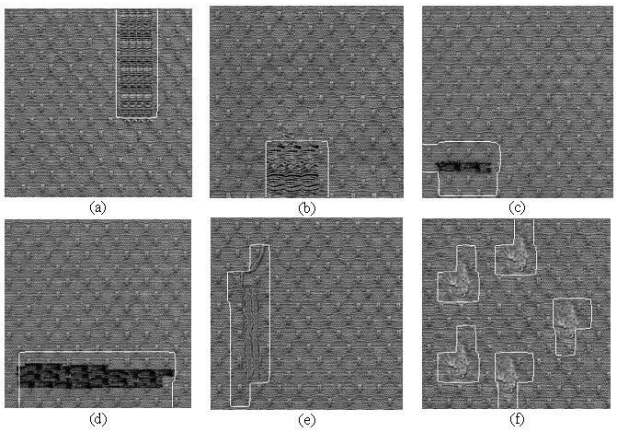

Figure 7: (a) Boundaries of the defective blocks identified from each cropped image shown superimposed on the original image; (b) Boundaries of the defective blocks shown separately on plain background; (c) Result of morphological filling; (d) Edges identified through Canny edge operator shown superimposed on original defective image using white pixels. Final result of defect identification after defect fusion, morphological filling and edge detection for (a) defective fabric image with broken end; (b) defective fabric image with hole; (c) defective fabric image with thin bar; (d) defective fabric image with thick bar; (e) defective fabric image with netting multiple; (f) defective fabric image with knot.

Table 1: Summary of performance parameters of the proposed algorithm.

Image defect	**Precision (%)**	**Recall (%)**	**Accuracy (%)**
Hole (in illustration)	100	82.1	95.6
Broken end	100	80.0	96.8
Hole	100	85.7	98.4
Thin bar	100	87.5	99.2
Thick bar	100	91.7	97.6
Netting multiple	100	77.5	97.2
Knot	100	80.4	95.6
Average	**100**	**83.6**	**97.2**

identified as defect-free. False positive is defined as the number of defect-free periodic blocks identified as defective. False negative is defined as the number of defective periodic blocks identified as defect-free. Precision is defined as the number of periodic blocks correctly labelled as belonging to the positive class divided by the total number of periodic blocks labelled as belonging to the positive class and is calculated as TP/(TP+FP). Recall is defined as the number of true positives divided by the sum of true positives and false negatives that are periodic blocks not labelled as belonging to the positive class but should have been and is calculated as TP/(TP+FN). Accuracy is the measure of success rate that takes into account the detection rates of defective and defect-free periodic blocks and is calculated as (TP+TN)/(TP+TN+FP+FN). These performance parameters are averaged for all cropped images and given in Table 1. The average precision, recall and accuracy for all the defective images (based on a total of 1764 number of periodic blocks) are 100%, 83.6%, and 97.2% respectively. The accuracy of a few other methods available in literature for defect detection on patterned textures varies from 88% to 99% [36]. Relatively less recall rates in the proposed method indicate that there are few false negatives identified by the proposed method. However, as the proposed method yields high precision and accuracy, the proposed method can contribute to automatic inspection in industries such as fabric industries. In general, the computational time complexity of a full GLCM is $O(M^2N^2)$. As the proposed method is based on reduced GLCM from 0-255 to 0-63, the time complexity is reduced by one-third.

3 Conclusion

In this paper, texture-periodicity and Jensen-Shannon divergence metrics have effectively been used for the development of the automated inspection on periodically patterned fabrics. Absence of training stage with defect-free test samples for obtaining decision-boundaries or thresholds, unsupervised method of identifying defects using cluster analysis, and high success rates are the novelties of the proposed method. Thus, the proposed method can contribute to the development of computerized inspection and quality control in industries such as fabric industries.

Acknowledgement

The author would like to thank Dr. Henry Y. T. Ngan, Research Assistant Professor, Department of Mathematics, Hong Kong Baptist University, Kowloon, for providing the database of patterned fabrics.

References

[1] H.Y.T Ngan, Pang and G.H.K. Regularity Analysis for Patterned Texture Inspection. IEEE Trans. Autom. Sci. Eng., Vol. 6 (1) (2009), pp. 131-144. (DOI: 10.1109/TASE.2008.917140)

[2] H.Y.T Ngan, Pang, G.H.K. and N.H.C Yung. Performance Evaluation for Motif-Based Patterned Texture Defect Detection. IEEE Trans. Autom. Sci. Eng. Vol. 7 (1) (2010) pp. 58-72. (DOI:10.1109/TASE.2008.2005418)

[3] H.Y.T Ngan, Pang and G.H.K. Novel method for patterned fabric inspection using Bollinger bands. Opt. Eng. Vol. 45 (8) (2006), pp. 087202-1-15. (DOI:10.1117/1.2345189)

[4] F Tajeripour, E Kabir and A Sheikhi. Fabric Defect Detection Using Modified Local Binary Patterns. In: Proc. of the Int. Conf. on Comput. Intel. And Multimed. Appl., (2007) pp. 261-267. (https://doi.org/10.1155/2008/783898)

[5] H.Y.T Ngan, Pang, G.H.K and N.H.C Yung. Motif-based defect detection for patterned fabric. Pattern

Recognit. Vol. 41, (2008), pp.1878-1894. (https://doi.org/10.1016/j.patcog.2007.11.014)

[6] H.Y.T Ngan, Pang, G.H.K. and N.H.C Yung. Ellipsoidal decision regions for motif-based patterned fabric defect detection. Pattern Recognit. Vol. 43, (2010) pp.2132-2144. (DOI:10.1016/j.patcog.2009.12.001)

[7] M.K Ng, H.Y.T Ngan, X.Yuan and W. Zhang. Patterned Fabric Inspection and Visualization by the Method of Image Decomposition. IEEE Trans. Autom. Sci. Eng. Vol. 11 (3) (2014), pp. 943-947. (DOI: 10.1109/TASE.2014.2314240)

[8] J Liang, C Chen, L. Jiuzhen, L and H Zhenjie. Fabric defect inspection based on lattice segmentation and Gabor filtering. Neurocomput. Vol. 238 (5), (2017), pp. 84-102. (https://doi.org/10.1016/j.neucom.2017.01.039)

[9] S Mei, Y. Wang, and G. Wen., Automatic Fabric Defect Detection with a Multi-Scale Convolutional Denoising Auto-encoder Network Model. Sensors. Vol. 18 (4), (2018), 1064-1074. (DOI:10.3390/s18041064)

[10] C. Li, G. Gao, Z. Liu, D. Huang and J Xi. Defect Detection for Patterned Fabric Images Based on GHOG and Low-Rank Decomposition. IEEE Access, Vol 7, (2019), pp. 83962-83973. DOI: 10.1109/ACCESS.2019.2925196

[11] R.A.L Morales, R.E.S Yanez and R.B. Serrato. Defect detection on patterned fabrics using texture periodicity and the coordinated clusters representation, Textile Research J., Vol 87 (15), (2016), pp. 1869-1882. https://doi.org/10.1177/0040517516660885

[12] V. Asha, N.U. Bhajantri and P. Nagabhushan. Automatic Detection of Defects on Periodically Patterned Textures, Journal of Intelligent Systems, vol. 20 (3), (2011), pp. 279-303. (https://www.degruyter.com/document/doi/10.1515/jisys.2011.015/html)

[13] V. Asha, N.U. Bhajantri and P. Nagabhushan. GLCM-based chi-square histogram distance for automatic detection of defects on patterned textures. International Journal of Computational Vision and Robotics (IJCVR), vol. 2 (4), (2011), pp. 302-313. (DOI: 10.1504/IJCVR.2011.045267)

[14] V. Asha, N.U. Bhajantri and P. Nagabhushan. Automatic Detection of Texture-defects using Texture-periodicity and Jensen-Shannon Divergence. Journal of Information Processing Systems, vol. 8 (2), (2012) pp. 359-374, 2012. (https://doi.org/10.3745/JIPS.2012.8.2.359)

[15] V. Asha, N.U. Bhajantri and P. Nagabhushan. Similarity measures for automatic defect detection on patterned textures. International Journal of Information and Communication Technology, vol. 4 (2/3/4), (2012), pp. 118-131. (https://www.inderscienceonline.com/doi/abs/10.1504/IJICT.2012.048758)

[16] V. Asha. Singular Value Decomposition of Images of Structural Textures and their Reconstruction using Periodicity. International Journal of Tomography and Simulation (IJTS), vol 31, Issue 4, (2018), pp 86-97. (http://www.ceser.in/ceserp/index.php/ijts/article/view/5696)

[17] V. Asha. Texture Defect Detection using Human Vision Perception based Contrast. International Journal of Tomography and Simulation (IJTS), vol 32, Issue 3, (2019), pp 86-97. (http://www.ceser.in/ceserp/index.php/ijts/article/view/6017)

[18] H. Jiang, Defect Features Recognition in 3D Industrial CT Images, Informatica – An Int. J. of Comput. and Inform., Vo. 42, No. 3 (2018). (https://doi.org/10.31449/inf.v42i3.2454)

[19] D.M Endres and J.E Schindelin. A New Metric for Probability Distributions. IEEE Trans. on Info. Theory, Vol 49 (7), (2003), pp.1858-1860. (DOI: 10.1109/TIT.2003.813506)

[20] T Caelli, B. Julesz and E. Gilbert. On Perceptual Analyzers Underlying Visual Texture Discrimination, Part II. Biol. Cybern. Vol 29(4), (1978), pp. 201-214. (DOI: 10.1007/BF00337138)

[21] R.M. Haralick, K. Shanmugam and I. Dinstein. Textural features for image classification. IEEE Trans. On Syst., Man and Cybern. Vol 3(6), (1973), pp. 610-621. (DOI:10.1109/TSMC.1973.4309314)

[22] R.M Haralick. Statistical and structural approaches to texture. In: Proc. of the IEEE, Vol 67(5), (1979) pp. 786 – 804. (DOI: 10.1109/PROC.1979.11328)

[23] A.L Amet, A. Ertuzun and A. Ercil. Texture defect detection using subband domain co-occurrence matrices. Image and Vis. Comp. Vol 18, (2000), pp. 543-553. (DOI: 10.1109/IAI.1998.666886)

[24] Fernandos, J.C.A., Neves, J.A.B.C, Couto and C.A.C. Defect Detection and Localization in Textiles using Co-occurrence Matrices and Morphological Operators. In:Proc. of the 6th Int.

Conf. onMechatron. Mach. Vis. In Pract. (M2VIP'99), Ankara, Turkey. (1999)

[25] C.F.J Kuo and T.L Su. Gray Relational Analysis for Recognizing Fabric Defects. Textile Res. J. Vol 73(5), (2003), pp. 461-465 (https://doi.org/10.1177/004051750307300515)

[26] L.H Soh and C Tsatsoulis. Texture Analysis of SAR SeaIce Imagery Using Gray Level Co-occurrence Matrices. IEEE Trans. On Geosci. Remote Sens. Vol 37(2), (1999), pp. 780-795. (DOI: 10.1109/36.752194)

[27] S. Theodoridis and K. Koutroumbas, Pattern Recognition, Fourth Edition, Academic Press, CA (2009)

[28] V. Asha, N.U. Bhajantri and P. Nagabhushan. Automatic Detection of Texture Defectsusing Texture-Periodicity and Gabor Wavelets. In: Venugopal, K.R., and Patnaik, L.M. (Eds.): ICIP 2011, Communication and Computer Information Series (CCIS) 157, Springer-Verlag, Berlin Heidelberg, (2011), pp. 548-553.

[29] V. Asha, P. Nagabhushan and N.U. Bhajantri. Automatic extraction of texture-periodicity using superposition of distance matching functions and their forward differences. Pattern Recog. Lett. 33 (5), (2012), pp. 629-640. (https://doi.org/10.1016/j.patrec.2011.11.027)

[30] R.C. Gonzalez, R.E. Woods. Digital Image Processing. Pearson Prentice Hall, New Delhi. (2008)

[31] J. Pisanki and T. Pisanki, The use of collaboration distance in scheduling conference talks, Informatica – An Int. J. of Comput. and Inform., Vo. 43, No. 4 (2019). (https://doi.org/10.31449/inf.v43i4.2832)

[32] T. Fawcett. An introduction to ROC analysis, Pattern Recognit. Lett. 27, (2006), pp. 861-874. (https://doi.org/10.1016/j.patrec.2005.10.010)

[33] C.D Brown and H.T. Davis. Receiver operating characteristics curves and related decision measures: A tutorial. Chemom. And Intell. Lab. Syst. 80, (2006), pp. 24-38. (https://doi.org/10.1016/j.chemolab.2005.05.004)

[34] E. K. Ampomah, Z. Qin, G. Nyame, F. E. Botchey, Stock market decision support modeling with tree-based AdaBoost ensemble machine learning models, Informatica – An Int. J. of Comput. and Inform., Vol. 44, No. 4 (2020). (https://doi.org/10.31449/inf.v44i4.3159)

[35] R. Patel, S. Tanwani, C. Patida, Relation Extraction between Medical Entities using Deep Learning Approach, Informatica – An Int. J. of Comput. and Inform., Vol. 45 No. 3 (2021). (https://doi.org/10.31449/inf.v45i3.3056)

[36] T. Czimmermann, G. Ciuti, M. Milazzo, M. Chiurazzi, S. Roccella, C.M. Oddo and P. Dario., Visual-Based Defect Detection and Classification Approaches for Industrial Applications—A SURVEY, Sensors 20, Article No. 1459. (DOI:10.3390/s20051459)